Supporting Information

Quenching of singlet oxygen as a decisive role in the efficiency and stability of ligand-protected Au cluster for photocatalytic oxidation

Wen-Wen Ren,[ab] Yuhsuan Lee,[c] Li-Jia Cao,[ab] Shu-Ming Bai,*[c] Song Gao,[dae] and Li-Nan Zhou*[abf]

a. Spin-X Institute, South China University of Technology, Guangzhou 511442, China;
b. School of Chemistry and Chemical Engineering, South China University of Technology, Guangzhou 510641, China;
c. Beijing National Laboratory for Molecular Sciences, State Key Laboratories for Structural Chemistry of Unstable and Stable Species, Institute of Chemistry, Chinese Academy of Sciences, Beijing 100190, China;
d. Key Laboratory of Bioinorganic and Synthetic Chemistry of Ministry of Education, School of Chemistry, LIFM, IGCME, GBRCE for Functional Molecular Engineering, Sun Yat-Sen University, Guangzhou 510275, China;
e. Beijing National Laboratory of Molecular Science, Beijing Key Laboratory of Magnetoelectric Materials and Devices, College of Chemistry and Molecular Engineering, Peking University, Beijing, 100871 China;
f. State Key Laboratory of Luminescent Materials and Devices, South China University of Technology, Guangzhou 510641, China.

* Corresponding authors.
E-mail address: zhoulinan@scut.edu.cn; baishuming@iccas.ac.cn

Content

Materials and methods

Materials

Tetrachloroauric(III) acid ($HAuCl_4 \cdot 3H_2O$, 98%), tetraoctylammonium bromide (TOAB, 99%), 2-phenylethanethiol (PET, 99%), sodium borohydride ($NaBH_4$, 99.99%), 2,2,6,6-tetramethylpiperidine (TEMP, 98%), 5,5-dimethyl-1-pyrroline N-oxide (DMPO, 97%), methyl phenyl sulfide (99%), methanol (HPLC grade, 99%), dichloromethane (HPLC grade, 99%), ethanol (HPLC grade, 99%), hexane (HPLC grade, 99.9%), toluene (HPLC grade, 99%). All reagents and solvents were commercially available and used without further purification unless otherwise noted. The purified water utilized in these processes has been treated with a water filtration system to ensure its quality. Furthermore, all glassware were thoroughly cleaned with aqua regia (HCl: HNO_3 = 3: 1 v/v), rinsed with copious amounts of pure water and then dried in an oven prior to use.

Synthesis of Au_{25} cluster

$[Au_{25}(PET)_{18}]^-$ clusters were synthesized according to the previously literature.[1] First, 524 mg $(C_8H_{17})_4NBr$ was added to THF (30 mL) containing 0.2956 g $HAuCl_4 \cdot 3H_2O$. The resulting solution was stirred for 15 min at room temperature and then 560 µL PhC_2H_4SH was added. The solution changed from clear red to colorless. After stirring for 60 min at room temperature, 10 mL iced water containing 284 mg $NaBH_4$ was quickly added to the solution. The solution rapidly became black, and was kept stirring at room temperature. After 12 h, the THF was evaporated and the remaining byproduct was washed with methanol more than three times. Single crystals were grown in mixed toluene and ethanol (1:4 v/v).

The cluster samples were then pipetted to TLC plates and dried in air. After drying, the plate was eluted with CH_2Cl_2/hexane mixture (For $[Au_{25}(PET)_{18}]^-$, the volume ratio of CH_2Cl_2/hexane is 60:40). After the separation, the bands were cut from the TLC plate, and the clusters from each band were individually extracted with CH_2Cl_2. The solids (pieces of TLC plate) were removed from these extracts by centrifugation.

Characterization

Electronic Spectroscopy

UV-visible absorption spectra were recorded on a Shimadzu UV-1900i spectrophotometer at room temperature. For analysis, the Au nanocluster samples were prepared as solutions in dichloromethane (CH_2Cl_2).

Matrix-assisted laser desorption/ionization time-of-flight mass spectrometry (MALDI-TOF MS)

MALDI-TOF MS was recorded on a Bruker Autoflex III smart beam instrument. Trans-2-[3-(4-tert-butylphenyl) -2-methyl-2-propenylidene] malononitrile (DCTB) was applied as a matrix. The matrix dissolved in CHCl3 at 4 mg·ml-1. $[Au_{25}(PET)_{18}]^-$ was dissolved in toluene at 4 mg·ml-1. Sample was prepared by depositing 0.5 uL of matrix on the wells of a 384-well ground-steel plate, allowing the spots to dry, depositing 0.5 uL of the $[Au_{25}(PET)_{18}]^-$ sample on a spot of dry matrix. The plate was inserted into the MALDI source after drying. Samples were tested in positive mode.

Single-crystal X-ray diffraction

Single-crystal diffraction data of $[Au_{25}(PET)_{18}]^-$ were collected using a Bruker SMART APEX II CCD diffractometer using graphite-monochromatized Mo Kα radiation (λ = 0.71073 Å) at 170 K. The data integration and reduction were processed using Olex2 software. After the initial structural model was generated using Olex2's AutoBuild tool, it was refined by SHELXL. In the process of refinement, the atomic coordinates and thermal vibration parameters were optimized, and a high-quality structural model was finally generated. The R factor after refinement was R1 = 0.0594 (9061), wR2 = 0.1579 (16697), and no significant problems were found in geometric inspection, indicating good structural stability.

Electron Paramagnetic Resonance (EPR)

EPR measurements were performed on a Bruker ESR 5000 spectrometer with a modulation amplitude of 0.1 G, a sweep time of 30 s, and a microwave power of 10 mW. To detect singlet oxygen, the spin-trapping agent TEMP was used. For this, two samples were prepared, each containing $[Au_{25}(PET)_{18}]^-$ (0.34 μM) and TEMP (0.078 M) in a 3 mL volume. The first sample was in a 14 wt% aqueous Triton X-100 solution, while the second was in CH_2Cl_2. For the detection of superoxide radicals, an analogous set of experiments was conducted. The spin trap DMPO was substituted for TEMP while keeping all other concentrations and conditions identical. All samples were irradiated for 10 min with an 805 nm LED before their spectra were recorded.

Photocatalytic measurements

Photocatalytic measurements were conducted in a batch reactor equipped with a commercial 805 nm LED as the light source. In a typical procedure, a reaction vial was charged with the substrate (150 μmol) and the $[Au_{25}(PET)_{18}]^-$ nanocluster catalyst (0.5 mol% relative to the substrate). The reaction medium was either CH_2Cl_2 (6 ml) or an aqueous micellar solution of 14 wt% Triton X-100 (6 ml). The vial was then sealed and the heterogeneous mixture was stirred vigorously at room temperature under an atmosphere of either ambient air or pure O_2. The reaction was irradiated for 8 hours. The progress of the reaction and the final yield were quantified by High-Performance Liquid Chromatography (HPLC) using a Thermo Scientific Acclaim™ 120 C18 column (5 μm, 120 Å, 4.6 × 250 mm) (see Figure S3-S13).

Catalyst Recovery Experiments

Upon completion of the reaction, water and saturated brine were added to the micellar reaction solution. The product was extracted into CH_2Cl_2, and the combined organic phases were concentrated under reduced pressure via rotary evaporation. The resulting sample was purified by washing with methanol to remove impurities. The gold nanoclusters were subsequently isolated by centrifugation, affording a recovery rate of 90%.

Kinetic Modeling

Under illumination, $Au_{25}(PET)_{18}^-$ nanoparticles undergo energy transfer with ground state molecular oxygen, leading to the generation of singlet oxygen (Eq. (i)), competing with the natural decay of excited Au cluster (Eq. (ii)).

$$^*Au_{25} \rightarrow Au_{25} \#(i)$$

$$^*Au_{25} + O_2 \rightarrow {}^1O_2 + Au_{25}\Phi_\Delta \#(ii)$$

The subsequent photophysical and photochemical processes of singlet oxygen are primarily governed by two steps:

$$2\ substrate + {}^1O_2 \xrightarrow{k_T} 2\ product\Phi_1 \#(iii)$$

$${}^1O_2 \xrightarrow{k_d} O_2 \#(iv)$$

$$\Phi_1 = \frac{k_T \times c_{substrate}}{k_T \times c_{subatrate} + k_d} \times 100\% \#(1)$$

Φ_1 represents the quenching efficiency of singlet oxygen by the substrate. k_T represents the second order rate constant of singlet oxygen reaction with substrate. k_d represents the decay rate constant of singlet oxygen in solvent. $c_{subatrate}$ represents the concentration of the substrate;

$$\Phi_{product} = \frac{N_{product}}{N_{photon}} \times 100\% \#(2)$$

$\Phi_{product}$ represents the quantum yield of the product; Φ_Δ represents the quantum yield of singlet oxygen.

Following Foote's kinetic quenching experiments[2] for singlet oxygen, a k_T value can be derived by reformulating the equation as follow:

$$\frac{1}{\Phi_{product}} = \frac{1}{\Phi_\Delta} \times \left(1 + \frac{k_d}{k_T} \times \frac{1}{c_{substrate}}\right) = \frac{1}{\Phi_\Delta} \times \frac{k_d}{k_T} \times \frac{1}{c_{substrate}} \times + \frac{1}{\Phi_\Delta} \#(3)$$

By conducting substrate concentration-dependent experiments and plotting the inverse of product

concentration against the inverse of substrate concentration, a linear curve can be fitted to the data with a slope of $\frac{1}{\Phi_\Delta} \times \frac{k_d}{k_T}$ and an intercept of $\frac{1}{\Phi_\Delta}$ (Figure 2(c) and 2(d)). bimolecular rate constant for the reaction between singlet oxygen and the substrate (k_T) can be obtained from the ratio of the slope (a) to the intercept (b) of this linear plot and the singlet oxygen decay rate constant (k_d, the lifetime of singlet oxygen ($^1O_2$) is solvent-dependent, with reported values of 25 μs in tert-butylbenzene and 95.7 μs in CH_2Cl_2[3]).

$$k_T = \frac{b}{a} \times k_d \#(4)$$

$$k_d = \frac{1}{\tau} \#(5)$$

Thus, for any given substrate concentration, the quenching efficiency of singlet oxygen by the substrate, Φ_1, can be obtained with equation (1)

The quantum yield of singlet oxygen Φ_Δ can be obtained by the quantum yield of the total quantity $\Phi_{product}$ and the quantum yield of the product Φ_1.

$$\Phi_\Delta = \frac{\Phi_{product}}{\Phi_1} \#(6)$$

Calculation of the apparent quantum yield of the product

The reaction apparatus is shown in Figure S9a. The incident light mostly impinges perpendicularly onto the reaction cuvette with known transmittance of ~90% and thus the number of absorbed photons (N_{photon}) can be calculated using the following equation, based on the incident light power (P) at 805 nm, which was measured using a commercial optical power meter (Thorlabs PM160T), and the absorbance of the reaction solution:

$$N_{photon} = \frac{P \cdot T \cdot t}{h \cdot \frac{c}{\lambda}} \times (1 - 10^{-A})$$

N_{photon}: the number of photons absorbed by the solution

P: the optical power of the incident light (W)

T: The transmittance of the reaction cuvette under 805nm light irradiation, which is 90%

t: the irradiation time (s)

λ: the wavelength of the light source (m)

h: Planck's constant

c: the speed of light

A: the absorbance of the solution at 805 nm

Estimation of effective volume of micelles

The effective total volume of the micelles ($V_{micelle}$) can be calculated as the product of the total number of micelles ($N_{micelle}$) and the average volume of a single micelle (V_{sphere}).

$$V_{micelle} = N_{micelle} \times V_{sphere}$$

Specifically, $N_{micelle}$ is estimated by dividing the total number of surfactant molecules by the mean aggregation number ($N_{aggregation}$), which represents the average number of surfactant monomers constituting a single micelle sphere. The volume of an individual micelle (V_{sphere}) is derived from the volume-weighted average radius (r).

$$N_{micelle} = \frac{n_{surfactant} \times N_A}{N_{aggregation}} = \frac{n_{surfactant} \times N_A}{\frac{M}{M_0}} = \frac{n_{surfactant} \times N_A \times M_0}{M}$$

$$V_{sphere} = \frac{4}{3}\pi r^3$$

Both of the M and r are determined via Dynamic Light Scattering (DLS). The monomer molecular weight (M_0) of Triton X-100 is 602.8 g·mol^{-1}.

The step-by-step calculation process is presented below:

$$V_{micelle} = N_{micelle} \times V_{sphere} = \frac{n_{surfactant} \times N_A \times M_0}{M} \times \frac{4}{3}\pi r^3 = \frac{14wt\% \times 1.05gcm^{-3}}{602.8g \cdot mol^{-1}}$$
$$\times \frac{4}{3}\pi(2.65nm)^3 \approx 5.522 \times 10^{18} \times 7.795 \times 10^{-23}dm^3 \approx 4.3 \times 10^{-4}dm^3 = 0.$$

DFT theoretical calculation

All density functional theory (DFT) Calculations were carried out with the Gaussian 16, Revision A.03. The M06-2x function and 6-311+g(d,p) basis set are used in our research. For all the calculations, Grimme-D3 correction was utilized for the empirical dispersion[4], and the solvent effect of DCM and heptane (Table S4) were included with Truhlar's SMD model[5].

Cartesian coordinates (Å) and energies of the optimized structures

MePhS_DCM

SCF energy: -669.700257499 a.u.

Free energy: -669.603034 a.u.

Cartesian Coordinates

ATOM X Y Z

S 1.82049400 -0.71978300 -0.00001000

C 2.69101600 0.86508300 0.00004400

C 0.11316600 -0.23669700 -0.00005000

H 2.46334700 1.44115900 -0.89673200

H 2.46311200 1.44119700 0.89673800

H 3.75240600 0.61562800 0.00019700

C -0.83361900 -1.26915700 -0.00001000

C -0.31974800 1.09005000 -0.00004200

C -2.18977800 -0.97381500 0.00002900

H -0.50510200 -2.30338100 -0.00001300

C -1.68478200 1.37481100 -0.00001100

H 0.38986500 1.90745900 -0.00004200

C -2.62458200 0.35122100 0.00002400

H -2.91024500 -1.78400500 0.00007300

H -2.00756800 2.40989300 -0.00001400

H -3.68374400 0.57960800 0.00005800

MePhS_heptane
SCF energy: -669.695915866 a.u.
Free energy: -669.598455 a.u.

Cartesian Coordinates
ATOM X Y Z
S 1.82024000 -0.71942400 -0.00049800
C 2.68752400 0.86548000 0.00089600
C 0.11457800 -0.23427200 -0.00022800
H 2.46238400 1.44326600 -0.89567500
H 2.46141600 1.44207000 0.89799700
H 3.74933500 0.61893000 0.00127700
C -0.83056300 -1.26719200 0.00019800
C -0.32211200 1.09034200 -0.00052600
C -2.18614600 -0.97496600 0.00038400
H -0.49815500 -2.29971700 0.00046000
C -1.68678500 1.37268100 -0.00024400
H 0.38506400 1.90936200 -0.00099400
C -2.62381700 0.34823400 0.00020800
H -2.90503600 -1.78615600 0.00074200
H -2.01183400 2.40679200 -0.00041300
H -3.68309500 0.57439900 0.00045200

TS-1_DCM
SCF energy: -819.954159580 a.u.
Free energy: -819.854582 a.u.

Cartesian Coordinates
ATOM X Y Z
O -1.85106000 1.28577300 -1.21836700
O -1.97101900 -0.02432000 -1.29331600
S -1.31433700 -0.91301200 0.26295200
C -2.08451300 0.19328600 1.43028600
H -3.05841100 -0.22948800 1.67267900
H -1.46766100 0.27782500 2.32335100
H -2.19369300 1.15730700 0.91735700
C 0.35748200 -0.36061500 0.21572100
C 1.30951200 -1.28827500 -0.21619800
C 0.70438300 0.96150800 0.49246300
C 2.62902100 -0.88450200 -0.36077200
H 1.02027600 -2.31102200 -0.43112400
C 2.03248400 1.34938000 0.34025100
H -0.03527700 1.67824500 0.82110300
C 2.98980000 0.43321600 -0.08296200

H 3.37530000 -1.59836600 -0.68783800
H 2.31463200 2.37359100 0.55276300
H 4.02185100 0.74448200 -0.19478700

TS-1_heptane
SCF energy: -819.943148010 a.u.
Free energy: -819.843307 a.u.

Cartesian Coordinates
ATOM X Y Z
O -1.94084800 1.37390600 -1.00787500
O -2.00081100 0.04844000 -1.22372600
S -1.30680600 -0.91706300 0.13695500
C -2.04325000 0.02394600 1.46278600
H -2.98973900 -0.45221100 1.71290100
H -1.37556000 0.04042800 2.32162800
H -2.20667600 1.02579000 1.03928500
C 0.36857500 -0.35988400 0.14778900
C 1.34052800 -1.28090600 -0.24554400
C 0.69279800 0.96530200 0.43637700
C 2.66303800 -0.87013600 -0.33426500
H 1.06349600 -2.30320000 -0.47655400
C 2.02208300 1.36083100 0.33514100
H -0.07434200 1.67533500 0.71169600
C 3.00194600 0.44922100 -0.04406500
H 3.42689500 -1.57850200 -0.63033500
H 2.28863400 2.38860400 0.54911700
H 4.03516000 0.76774700 -0.11551800

IM_DCM
SCF energy: -819.959333201 a.u.
Free energy: -819.858383 a.u.

Cartesian Coordinates
ATOM X Y Z
O -1.94142600 1.31916600 -1.11096400
O -2.05374500 -0.11159800 -1.12639200
S -1.33389300 -0.81905100 0.13812400
C -2.00620100 0.07842400 1.53510400
H -3.02736200 -0.27710100 1.66937000
H -1.39736200 -0.16129600 2.40674400
H -1.98918900 1.13956500 1.29348900
C 0.36217300 -0.29330000 0.10798300
C 1.29270300 -1.27975600 -0.21376300

C 0.74036000 1.02662800 0.35231400
C 2.63831300 -0.93684100 -0.28620700
H 0.97288300 -2.29877800 -0.40187000
C 2.08855300 1.35222100 0.27068100
H 0.00110300 1.78142400 0.58105100
C 3.03191400 0.37580100 -0.04548700
H 3.37337400 -1.69393700 -0.53019600
H 2.40233200 2.37341500 0.45044600
H 4.08098300 0.64192000 -0.10392600

IM_heptane
SCF energy: -819.945361627 a.u.
Free energy: -819.845527 a.u.

Cartesian Coordinates
ATOM X Y Z
O -2.00181200 1.44532500 -0.84504100
O -2.07889800 0.03885300 -1.10554800
S -1.32505300 -0.84840900 0.01332600
C -1.95737500 -0.15002900 1.54098200
H -2.95977800 -0.55122700 1.68394600
H -1.29662900 -0.45081000 2.35251800
H -1.98898700 0.93028400 1.39627300
C 0.36831500 -0.30620100 0.04358300
C 1.32419100 -1.26744300 -0.27741800
C 0.71725700 1.01207500 0.33656400
C 2.66589600 -0.90479600 -0.29094000
H 1.02516700 -2.28255700 -0.51336600
C 2.06225000 1.35855700 0.30709000
H -0.05170700 1.74388600 0.54077900
C 3.03073700 0.40553600 0.00018800
H 3.42065800 -1.64271300 -0.53293500
H 2.35339600 2.37999700 0.51942800
H 4.07679500 0.68805700 -0.01544300

TS-2_DCM
SCF energy: -1489.64741835 a.u.
Free energy: -1489.428309 a.u.

Cartesian Coordinates
ATOM X Y Z
O -2.07472300 1.50775500 -1.15132100
S -2.91932700 0.43274900 -0.40627900
C -3.26828100 1.17238300 1.19179100

H -4.01677800 1.94411700 1.01316000
H -3.66683500 0.40295100 1.85304000
H -2.34348600 1.61033000 1.56346600
C -1.82966100 -0.91650100 0.05150400
C -1.93911800 -2.06560700 -0.72702600
C -0.92761000 -0.83783000 1.11024900
C -1.12722100 -3.16002900 -0.44113900
H -2.65017700 -2.10812100 -1.54529600
C -0.13321300 -1.94173800 1.39464200
H -0.83071900 0.07392600 1.68472800
C -0.23055000 -3.09729100 0.62058200
H -1.20211700 -4.05780400 -1.04291200
H 0.57393200 -1.89487900 2.21469600
H 0.39954900 -3.95027100 0.84614700
O -0.69586700 1.88258700 -0.20325700
S 1.30321800 2.18756700 0.70821900
C 1.77362300 3.28360400 -0.65216900
C 1.97995100 0.64135800 0.12551000
H 2.85781200 3.33000400 -0.75459300
H 1.30105100 2.93071300 -1.56723400
H 1.38323800 4.27152600 -0.40564200
C 2.93583300 -0.02555500 0.88849800
C 1.51265300 0.07998100 -1.06539800
C 3.42566400 -1.25974100 0.46051700
H 3.29502800 0.41574000 1.81168000
C 2.02127700 -1.13932700 -1.49607200
H 0.72869000 0.59213300 -1.61135400
C 2.97484800 -1.81405900 -0.73250200
H 4.16574400 -1.77952100 1.05858000
H 1.65823200 -1.57564600 -2.42019700
H 3.36011200 -2.77087400 -1.06661200

TS-2_heptane
SCF energy: -1489.63610315 a.u.
Free energy: -1489.415856 a.u.

Cartesian Coordinates
ATOM X Y Z
O -2.03743600 1.49998500 -1.15993400
S -2.89687000 0.44925900 -0.40895100
C -3.21984900 1.21403000 1.18654000
H -3.98275200 1.97233600 1.01335800
H -3.58442600 0.45576600 1.87870600
H -2.28795600 1.67749500 1.50911600

C -1.83042100 -0.91452600 0.06537200
C -1.97933900 -2.08006700 -0.68038500
C -0.89508000 -0.82555300 1.09344600
C -1.17487600 -3.17902300 -0.39409000
H -2.71425600 -2.12870300 -1.47664800
C -0.10571600 -1.93231100 1.37736800
H -0.76282900 0.10308700 1.63252500
C -0.24249300 -3.10305300 0.63446900
H -1.28029000 -4.08934200 -0.97166000
H 0.63477800 -1.87261700 2.16604100
H 0.38749100 -3.95669100 0.85641800
O -0.67934700 1.86994200 -0.18677700
S 1.31481000 2.18216900 0.71942700
C 1.71942500 3.27774900 -0.66147100
C 1.97844200 0.63751000 0.11750700
H 2.79761700 3.33037900 -0.81148400
H 1.20128500 2.92148900 -1.54961100
H 1.33121800 4.26174200 -0.39809000
C 2.95444700 -0.02688700 0.85634400
C 1.47744800 0.07085300 -1.05693400
C 3.43064500 -1.26347600 0.42234900
H 3.34007300 0.42269300 1.76453300
C 1.97366600 -1.15054700 -1.49407200
H 0.67496300 0.57987000 -1.57874600
C 2.94656400 -1.82268900 -0.75455100
H 4.18829700 -1.78007300 1.00061000
H 1.58417800 -1.59111900 -2.40501000
H 3.32265400 -2.78063300 -1.09534700

MePhSO_DCM
SCF energy: -744.875640361 a.u.
Free energy: -744.775991 a.u.

Cartesian Coordinates
ATOM X Y Z
O -2.18509800 1.30015700 -0.26744700
S -1.66680000 -0.11261700 -0.46707400
C -2.07729800 -1.01247800 1.04744900
H -3.16253600 -1.11593300 1.06988400
H -1.60657700 -1.99597800 1.01680200
H -1.72471900 -0.43065100 1.89991300
C 0.11961600 -0.04450300 -0.20218600
C 0.88663700 -1.18864100 -0.40219400
C 0.69105200 1.16551200 0.16216600

C 2.26187700 -1.11614700 -0.21009500
H 0.42305000 -2.12187100 -0.70710800
C 2.07075700 1.22644000 0.34859900
H 0.05922300 2.03733700 0.29005200
C 2.85239000 0.08971700 0.16609900
H 2.87274800 -1.99861900 -0.35992400
H 2.53294200 2.16436900 0.63390600
H 3.92526500 0.14256700 0.31020500

MePhSO_heptane
SCF energy: -744.868320173 a.u.
Free energy: -744.768358 a.u.

Cartesian Coordinates
ATOM X Y Z
O -2.18196100 1.29157600 -0.27466500
S -1.66961300 -0.11565500 -0.46957400
C -2.06841200 -1.00542700 1.05932400
H -3.15342800 -1.10589800 1.09203100
H -1.59836400 -1.98929100 1.04218300
H -1.71331600 -0.41243200 1.90267100
C 0.11899800 -0.05168800 -0.20418700
C 0.89371100 -1.18947300 -0.40528700
C 0.68291300 1.16075500 0.16175800
C 2.26767400 -1.11023800 -0.21098300
H 0.43632200 -2.12309600 -0.71790400
C 2.06110800 1.22905600 0.35069900
H 0.04031200 2.02572900 0.28454900
C 2.84960900 0.09777200 0.16861000
H 2.88471100 -1.98780300 -0.36296200
H 2.51787700 2.16919500 0.63658400
H 3.92177100 0.15692800 0.31375500

$^1O_2$_DCM
SCF energy: -150.249697012 a.u.
Free energy: -150.264576 a.u.

$^1O_2$_heptane
SCF energy: -150.250549728 a.u.
Free energy: -150.265433 a.u.

Supplementary Figures and Tables

Table S1 Crystal data and structure refinement for $Au_{25}(PET)_{18}$.

Empirical formula	$C_{144}H_{162}Au_{25}S_{18}$
Formula weight	7393.97
Temperature/K	170.0
Crystal system	triclinic
Space group	P-1
a/Å	16.190(2)
b/Å	17.380(3)
c/Å	18.693(2)
α/°	106.207(4)
β/°	105.827(4)
γ/°	91.014(4)
Volume/Å^3	4834.1(12)
Z	1
ρ_{calc}g/cm^3	2.540
μ/mm^{-1}	19.111
F (000)	3289.0
Crystal size/mm^3	0.11 × 0.05 × 0.02
Radiation	MoKα (λ = 0.71073)
2Θ range for data collection/°	3.882 to 50.182
Index ranges	-19 ≤ h ≤ 19, -20 ≤ k ≤ 20, -22 ≤ l ≤ 19
Reflections collected	44884
Independent reflections	16697 [R_{int} = 0.0958, R_{sigma} = 0.1188]
Data/restraints/parameters	16697/1228/820
Goodness-of-fit on F^2	0.959
Final R indexes [I>=2σ (I)]	R_1 = 0.0594, wR_2 = 0.1288
Final R indexes [all data]	R_1 = 0.1224, wR_2 = 0.1579
Largest diff. peak/hole / e Å^{-3}	2.43/-1.26

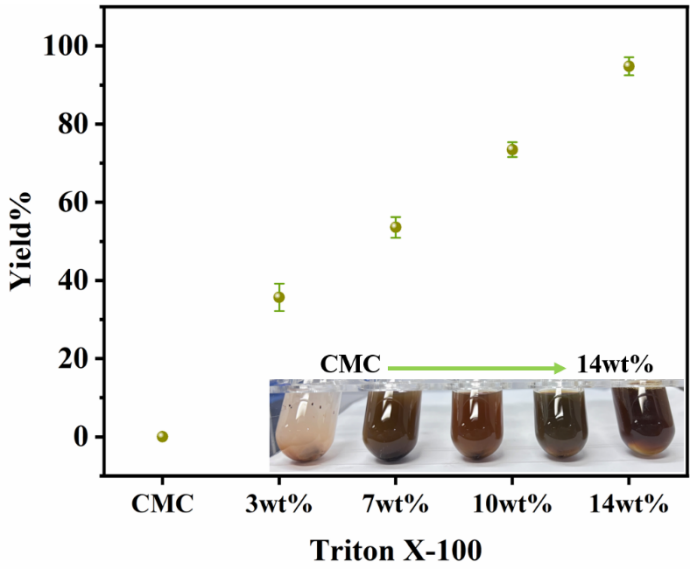

Figure S1 The yield of the photocatalytic oxidation of Methylphenylsulfide using Au_{25} cluster in different micelle concentrations after 8 hours.

Table S2 Detailed comparison of sustainability metrics including E-factor, waste generation, and energy efficiency for the reaction in Triton X-100 versus CH_2Cl_2.

Parameter	Triton X-100	CH_2Cl_2
Reaction time (h)	8	8
Theoretical yield (mg)	21.6	21.6
Actual yield (mg)	20.5	2.4
Waste (g)	168.1	52.9
E-factor (10^3)	8.2	22
Energy input (W•h)	64	64
Energy consumption (Wh/g)	3121.9	26666.7

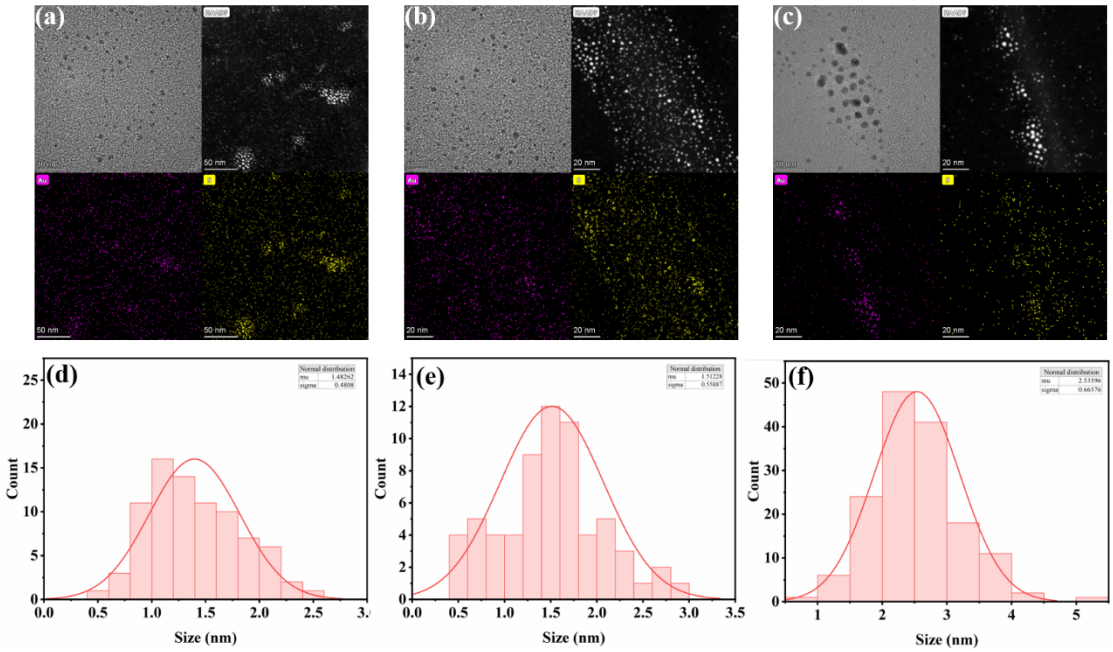

Figure S2 Characterization of the catalyst before and after the reaction. (a-c) TEM images of (a) the fresh Au_{25} catalyst, (b) the recovered catalyst in Triton X-100 after four reaction cycles, and (c) the recovered catalyst in CH_2Cl_2. (d-f) Corresponding particle size distribution histograms of (d) the fresh Au_{25} catalyst, (e) the recovered catalyst in Triton X-100 after four reaction cycles, and (f) the recovered catalyst in CH_2Cl_2.

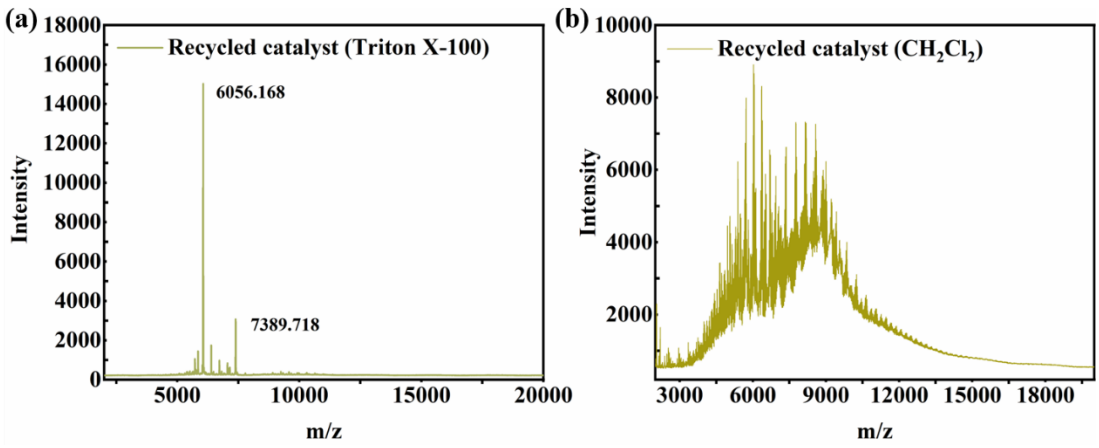

Figure S3 MALDI-TOF MS spectra of (a) the recovered catalyst in Triton X-100 after four reaction cycles and (b) the recovered catalyst in CH_2Cl_2.

Table S3 ICP-OES results of Au and S mass fractions in the catalysts before and after four reaction cycles.

Sample	Au mass fration (%)	S mass fration (%)
Fresh catalyst	60.4651	7.4169
Catalyst after 4cycles	58.3452	5.1918

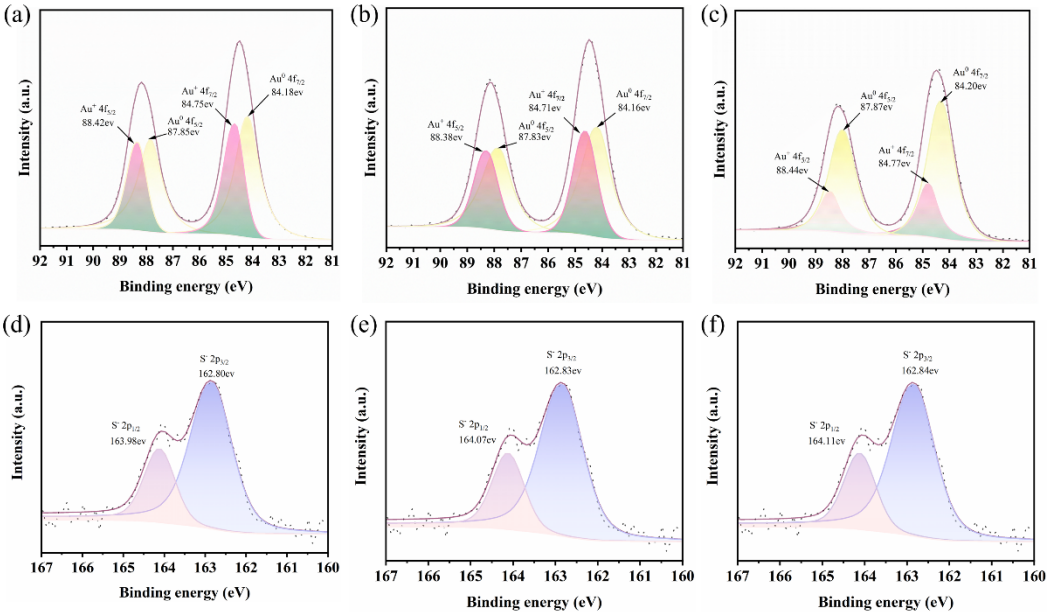

Figure S4 XPS spectra of the catalyst. (a-c) Au 4f regions of (a) the fresh catalyst, (b) the recovered catalyst in Triton X-100 after four reaction cycles, and (c) the recovered catalyst in CH_2Cl_2. (d-f) S 2p regions of (d) the fresh catalyst, (e) the recovered catalyst in Triton X-100 after four reaction cycles, and (f) the recovered catalyst in CH_2Cl_2.

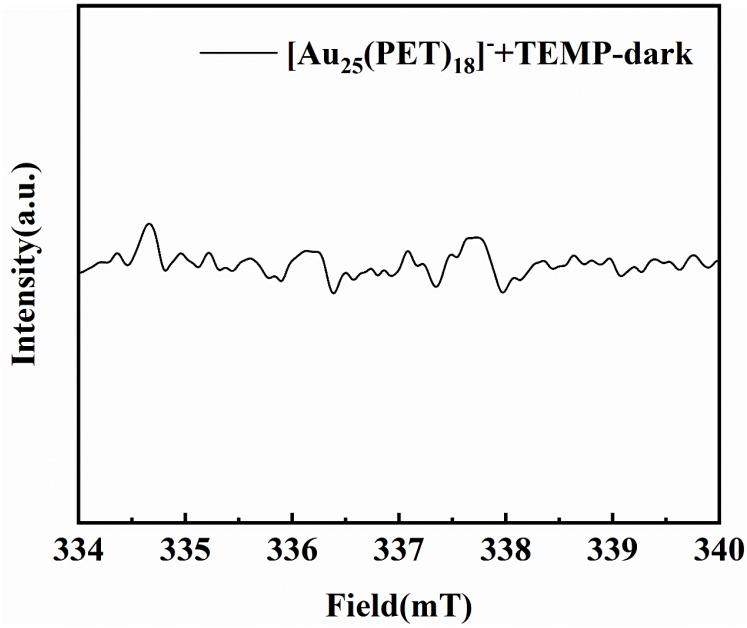

Figure S5 the EPR signal generated by adding TEMP to the $[Au_{25}(PET)_{18}]^-$ solution under dark conditions.

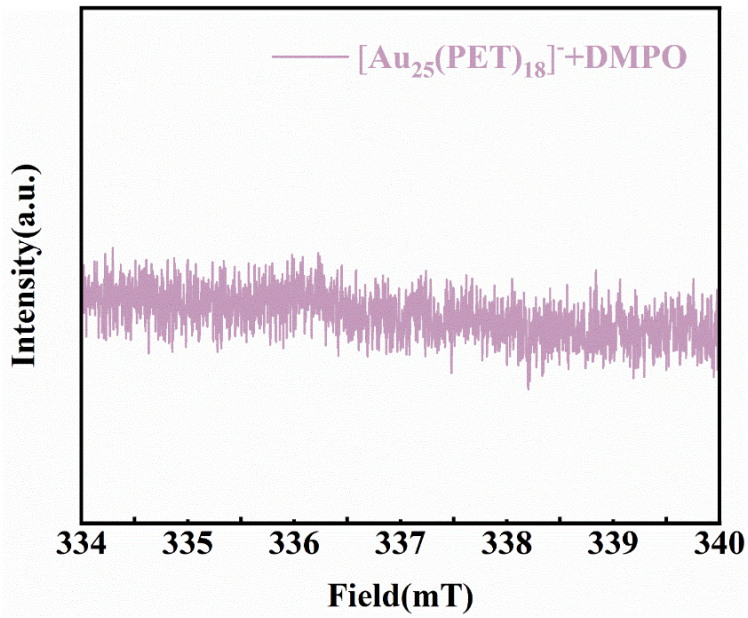

Figure S6 the EPR signal produced by adding DMPO to the $[Au_{25}(PET)_{18}]^-$ solution.

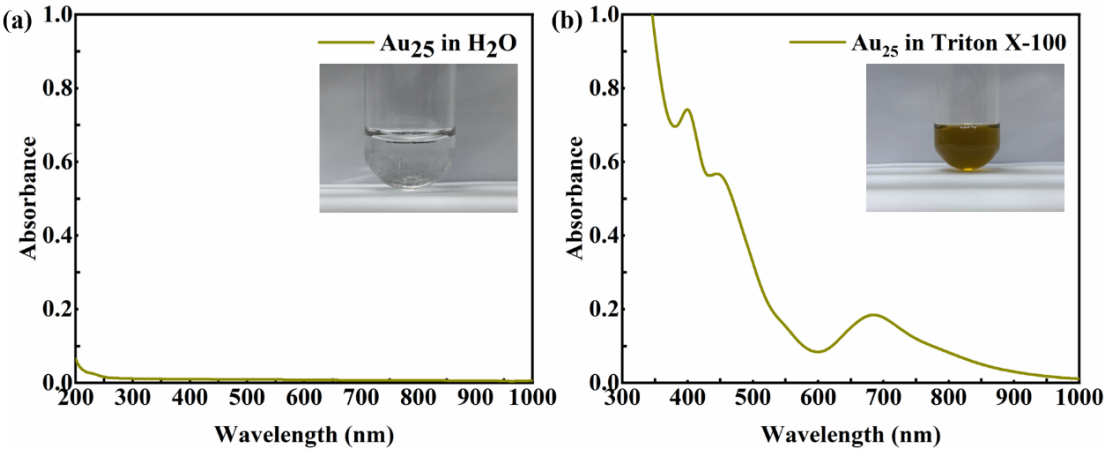

Figure S7 (a) Au_{25} is insoluble in water; (b)Au_{25} dissolves in Triton X-100.

Note: The insolubility of Au_{25} clusters in water suggests that they must be encapsulated within the micelles to remain in solution. UV-Vis absorption spectra confirm this effective encapsulation, as shown by the characteristic absorbance features appearing only in the presence of Triton X-100 (Figure S7).

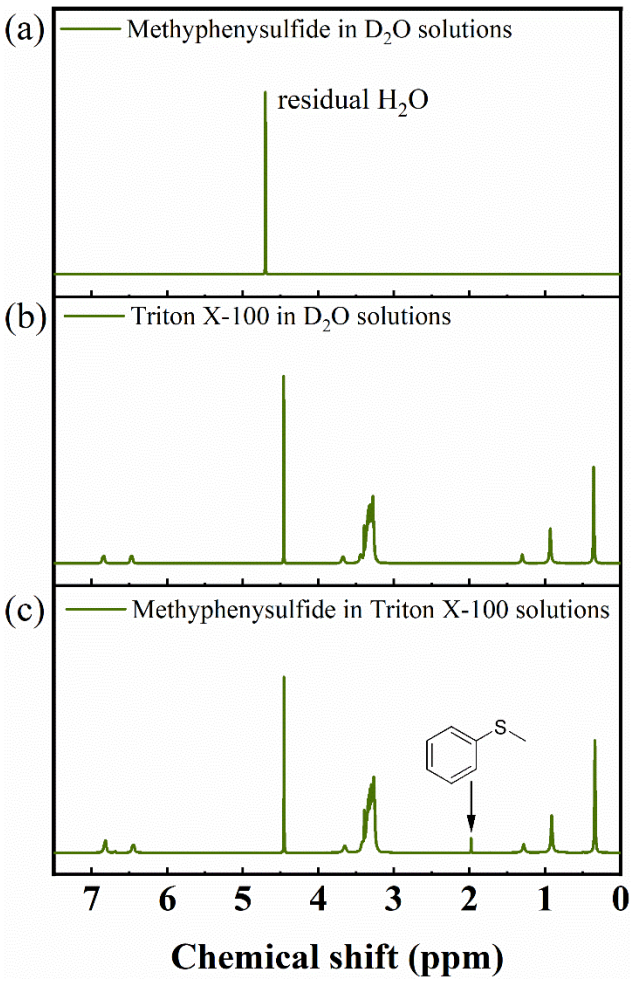

Figure S8 1H NMR Spectrum of (a) Methyphenysulfide in D_2O; (b) Triton X-100 in D_2O; and (c) Methyphenysulfide in Triton X-100 solutions (D_2O as solvent).

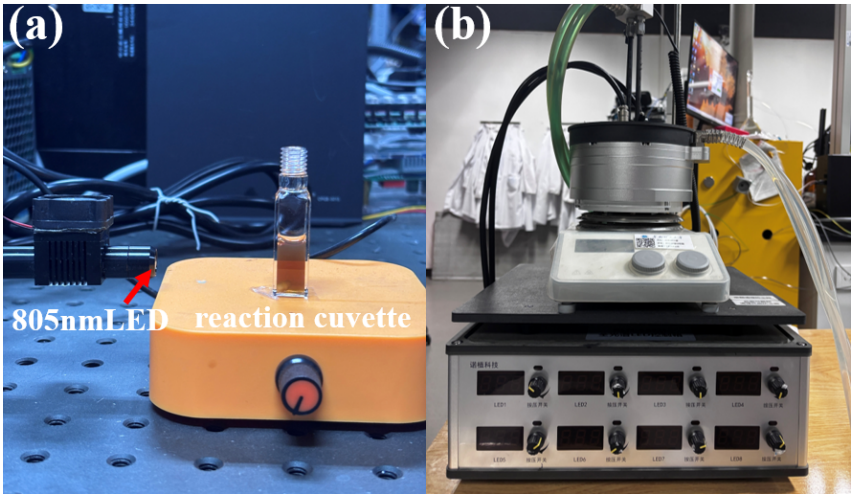

Figure S9 Experimental apparatus used in this study. (a) Setup for singlet oxygen quantum yield measurements (or kinetic studies). (b) The reactor system used for the photooxidation of Methylphenylsulfide.

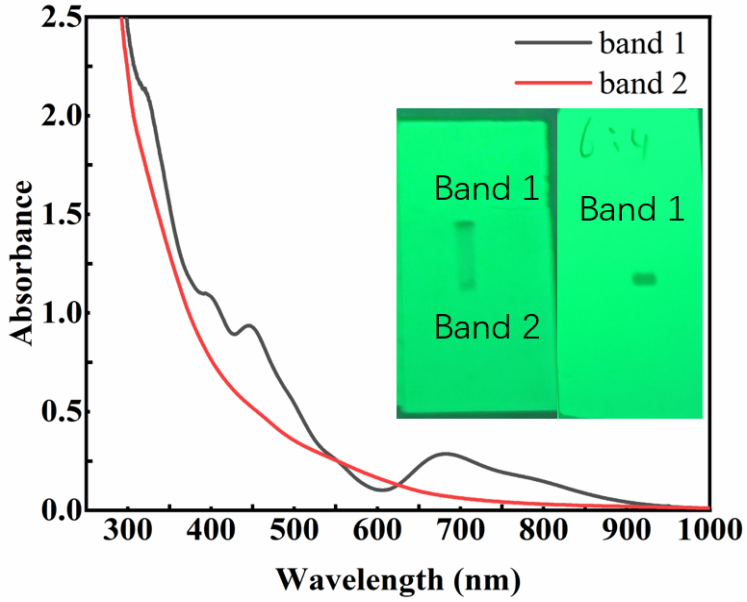

Figure S10 The target cluster was separated by silica gel column chromatography.

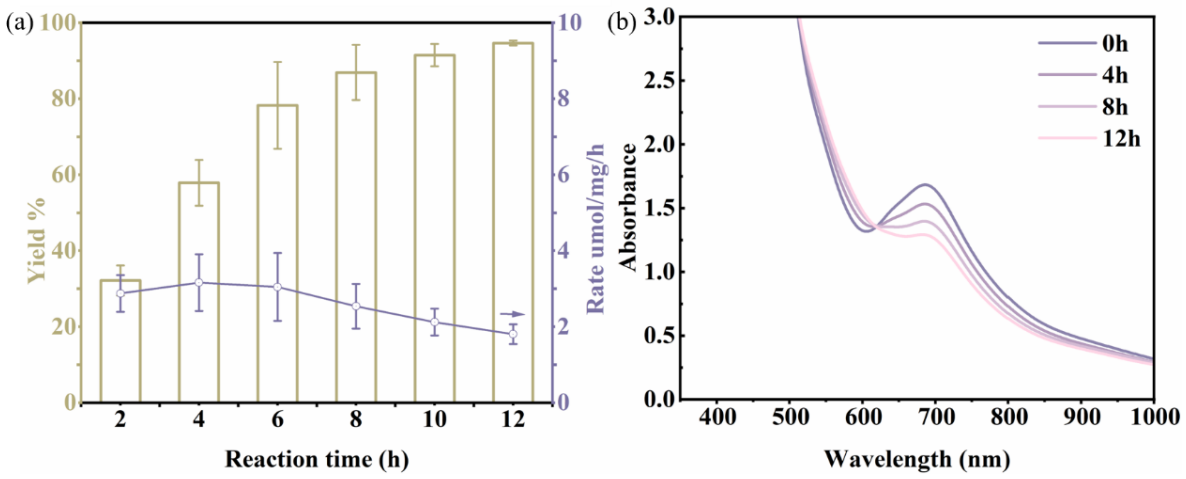

Figure S11 (a) Yield and reaction rate of the photooxidation of Methylphenylsulfide in a micellar solution containing CH_2Cl_2; (b) UV-vis absorption spectra monitored during the photooxidation of Methylphenylsulfide in a micellar solution containing CH_2Cl_2.

Table S4 ε values for different solvents from the Gaussian SCRF Solvent Database (https://gaussian.com/scrf/).

 n-Pentane varepsilon=1.8371	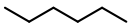 n-Hexane varepsilon=1.8819	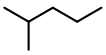 2-MethylPentane varepsilon=1.89	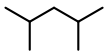 2,4-DiMethylPentane varepsilon=1.8939
 Heptane varepsilon=1.9113	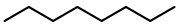 n-Octane varepsilon=1.9406	 n-Nonane varepsilon=1.9605	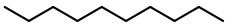 n-Decane varepsilon=1.9846
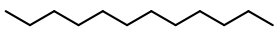 n-Dodecane varepsilon=2.0060	 Water varepsilon=78.3553	 Dichloromethane varepsilon=8.93	

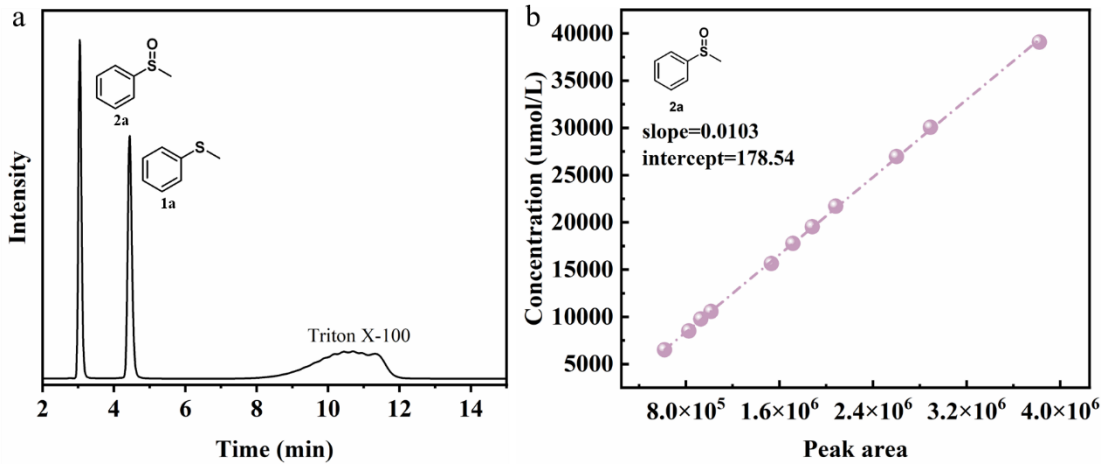

Figure S12 Identification and quantification of product 2a by High-Performance Liquid Chromatography. (a) The representative HPLC chromatogram of reagent sulfide 1a and its corresponding product sulfoxide 2a. (b) The standard calibration curve, constructed by plotting integrated peak area against concentrations of 2a.

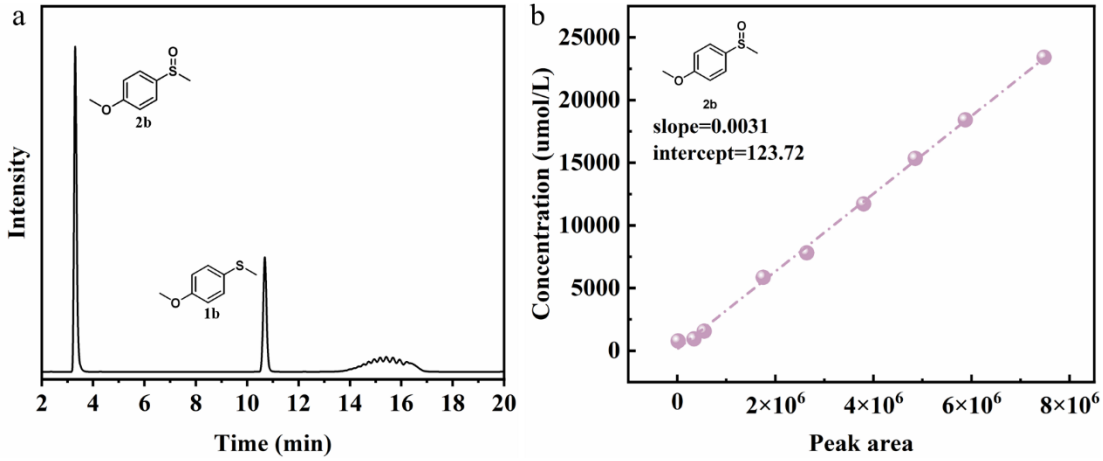

Figure S13 Identification and quantification of product 2b by High-Performance Liquid Chromatography. (a) The representative HPLC chromatogram of reagent sulfide 1b and its corresponding product sulfoxide 2b. (b) The standard calibration curve, constructed by plotting integrated peak area against concentrations of 2b.

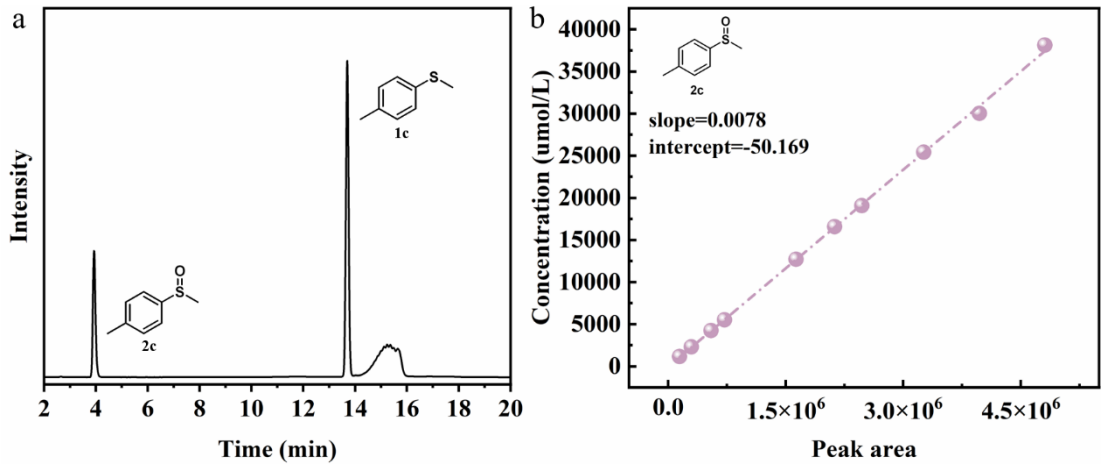

Figure S14 Identification and quantification of product 2c by High-Performance Liquid Chromatography. (a) The representative HPLC chromatogram of reagent sulfide 1c and its corresponding product sulfoxide 2c. (b) The standard calibration curve, constructed by plotting integrated peak area against concentrations of 2c.

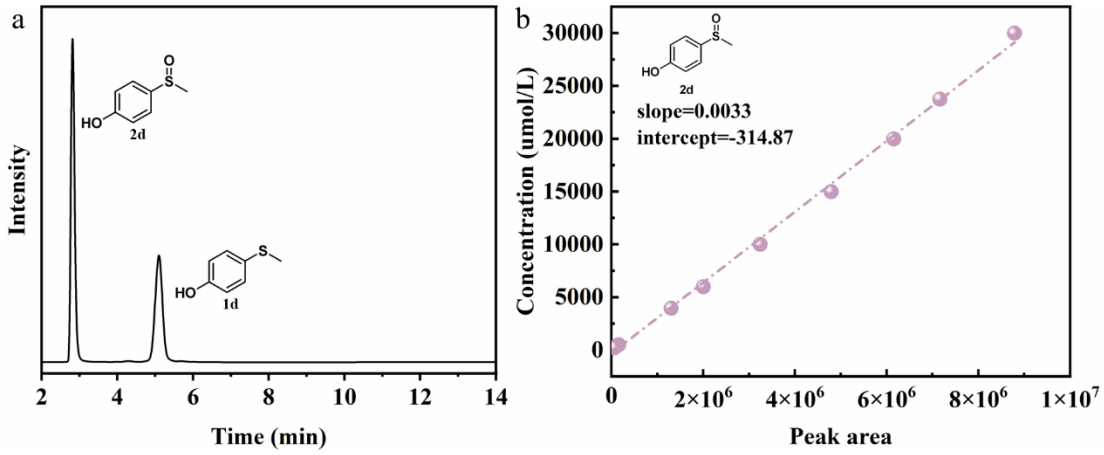

Figure S15 Identification and quantification of product 2d by High-Performance Liquid Chromatography. (a) The representative HPLC chromatogram of reagent sulfide 1d and its corresponding product sulfoxide 2d. (b) The standard calibration curve, constructed by plotting integrated peak area against concentrations of 2d.

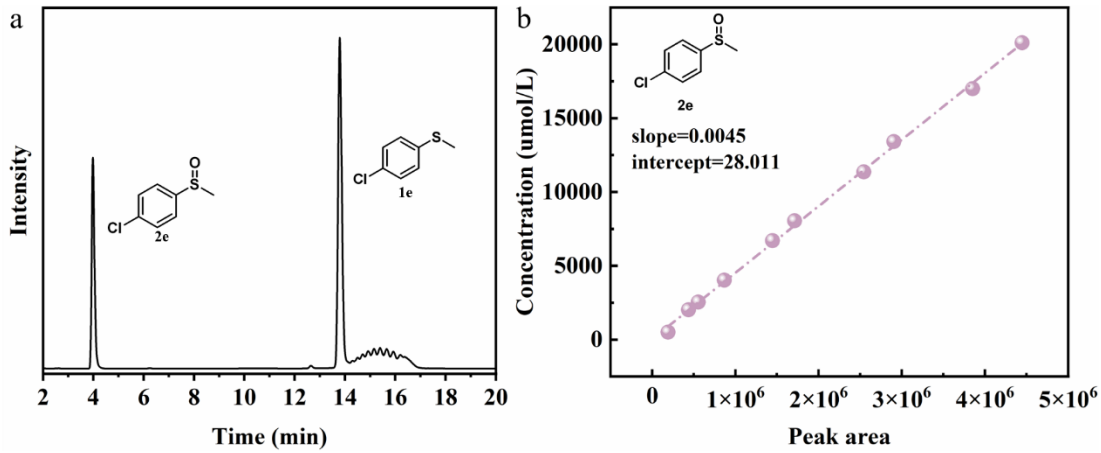

Figure S16 Identification and quantification of product 2e by High-Performance Liquid Chromatography. (a) The representative HPLC chromatogram of reagent sulfide 1e and its corresponding product sulfoxide 2e. (b) The standard calibration curve, constructed by plotting integrated peak area against concentrations of 2e.

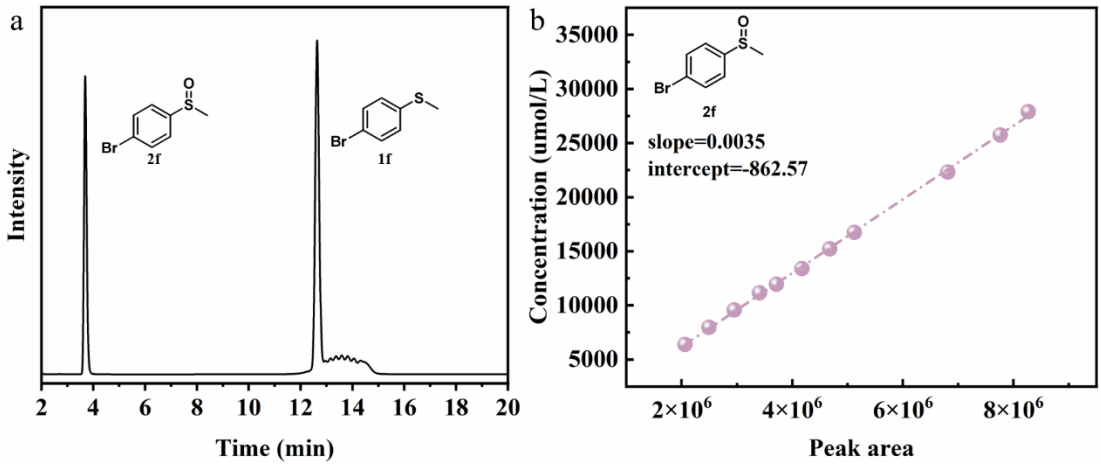

Figure S17 Identification and quantification of product 2f by High-Performance Liquid Chromatography. (a) The representative HPLC chromatogram of reagent sulfide 1f and its corresponding product sulfoxide 2f. (b) The standard calibration curve, constructed by plotting integrated peak area against concentrations of 2f.

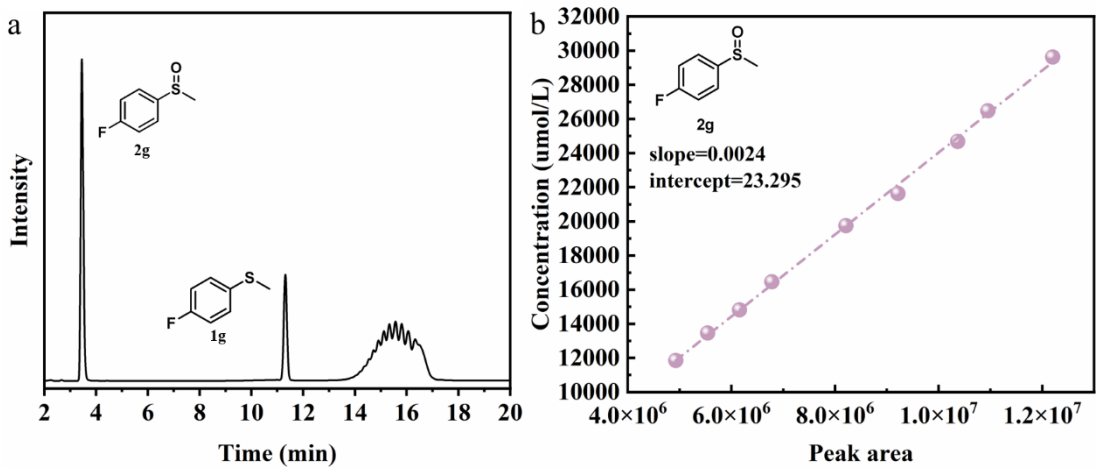

Figure S18 Identification and quantification of product 2g by High-Performance Liquid Chromatography. (a) The representative HPLC chromatogram of reagent sulfide 1g and its corresponding product sulfoxide 2g. (b) The standard calibration curve, constructed by plotting integrated peak area against concentrations of 2g.

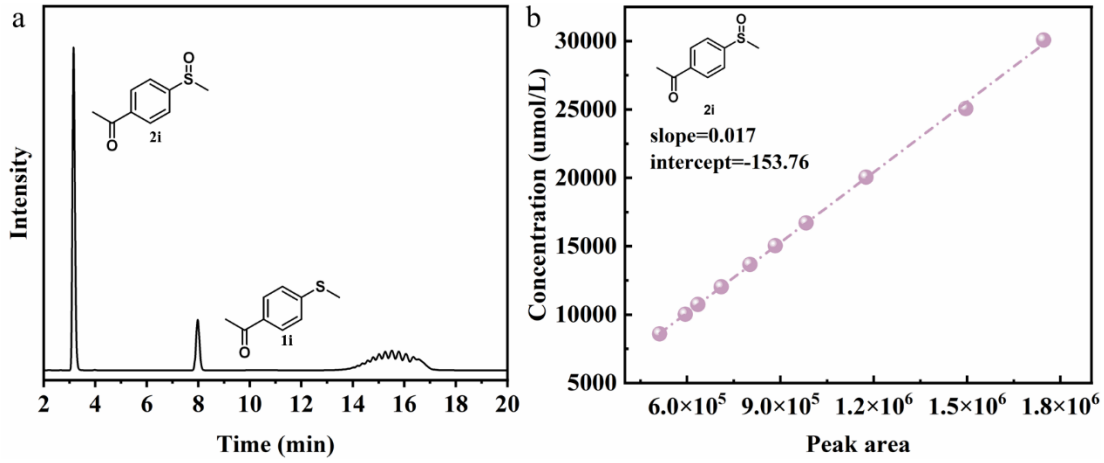

Figure S19 Identification and quantification of product 2i by High-Performance Liquid Chromatography. (a) The representative HPLC chromatogram of reagent sulfide 1i and its corresponding product sulfoxide 2i. (b) The standard calibration curve, constructed by plotting integrated peak area against concentrations of 2i.

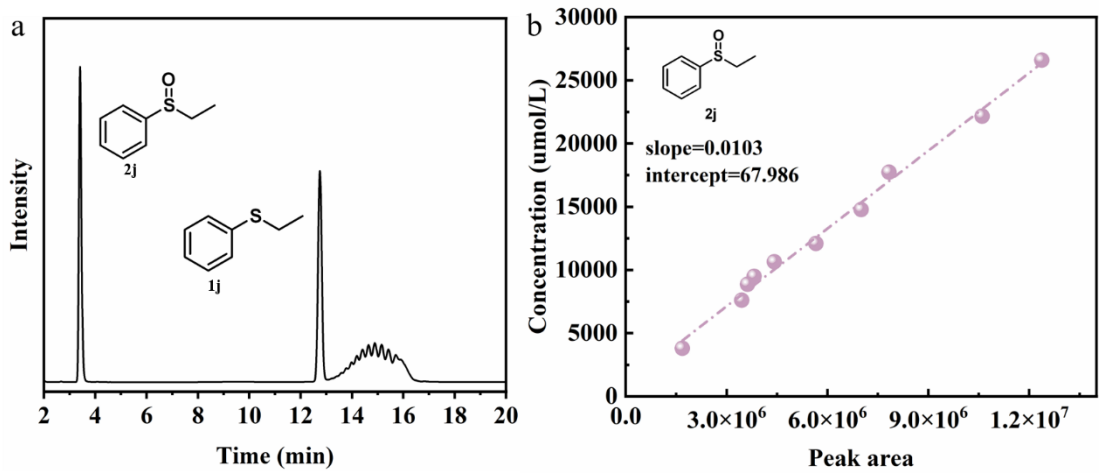

Figure S20 Identification and quantification of product 2j by High-Performance Liquid Chromatography. (a) The representative HPLC chromatogram of reagent sulfide 1j and its corresponding product sulfoxide 2j. (b) The standard calibration curve, constructed by plotting integrated peak area against concentrations of 2j.

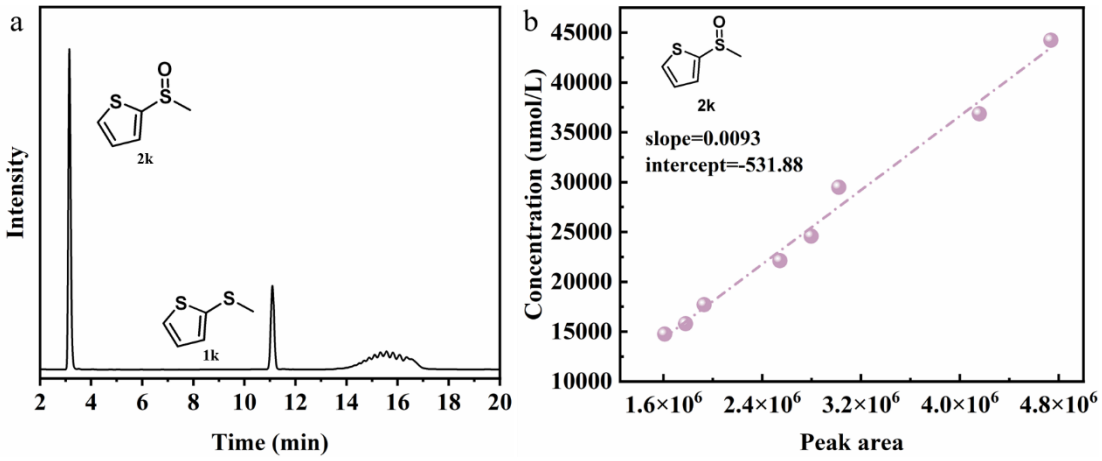

Figure S21 entification and quantification of product 2k by High-Performance Liquid Chromatography. (a) The representative HPLC chromatogram of reagent sulfide 1k and its corresponding product sulfoxide 2k. (b) The standard calibration curve, constructed by plotting integrated peak area against concentrations of 2k.

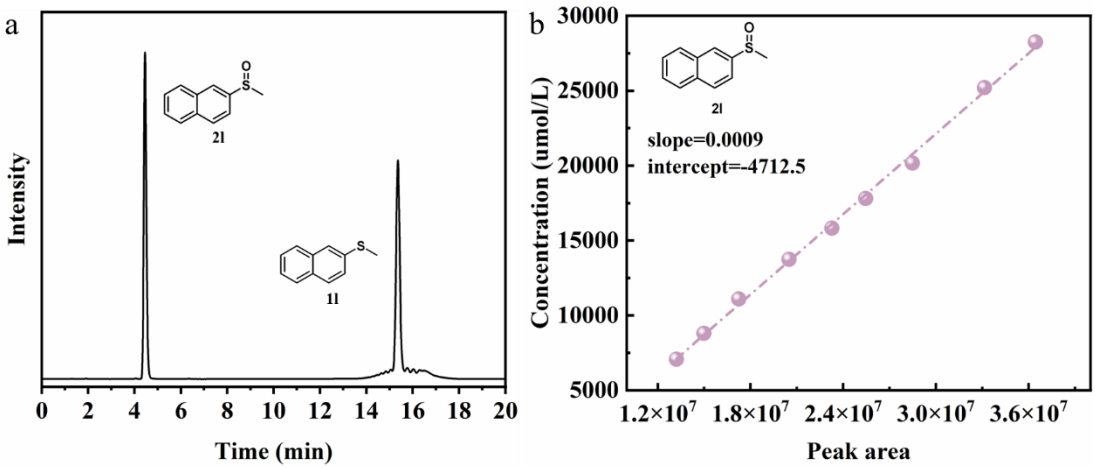

Figure S22 Identification and quantification of product 2l by High-Performance Liquid Chromatography. (a) The representative HPLC chromatogram of reagent sulfide 1l and its corresponding product sulfoxide 2l. (b) The standard calibration curve, constructed by plotting integrated peak area against concentrations of 2l.

Table S5 The information of purchased sulfides and sulfoxides

Material	CAS	Trademark	Parameters/indicators
Methyphenylsulfide	100-68-5	Adamas	99%
Methyphenylsulfoxide	1193-82-4	Adamas	98%+
4-Methoxythioanisole	1879-16-9	Adamas	98%+
1-Methoxy-4-(methylsulfinyl)benzene	3517-99-5	Adamas	97%
Methylp-tolylsulfide	623-13-2	Adamas	99%
1-Methyl-4-(methylsulfinyl)benzene	934-72-5	Adamas	98%+
4-(Methylthio)phenol	1073-72-9	Adamas	98%+
4-(Methylsulfinyl)phenol	14763-64-5	Adamas	98%
4-Chlorothioanisole	123-09-1	Adamas	98%+
1-Chloro-4-(methylsulfinyl)benzene	934-73-6	Adamas	99%+
4-Bromothioanisole	104-95-0	Adamas	98%+
1-Bromo-4-(methylsulfinyl)benzene	934-71-4	Adamas	98%
4-Fluorothioanisole	371-15-3	Adamas	98%+
1-Fluoro-4-(methylsulfinyl)benzene	658-14-0	Adamas	95%
1-(4-(Methylthio)phenyl)ethanone	1778-09-2	Adamas	98%+
1-(4-Methanesulfinylphenyl)ethan-1-one	32361-73-2	Bidepharm	95%
EthylPhenylSulfide	622-38-8	Adamas	98%
(Ethylsulfinyl)benzene	4170-80-3	Adamas	95%
2-(Methylthio)thiophene	5780-36-9	Adamas	99%+

2-(Methylsulfinyl)thiophene	74166-42-0	Bidepharm	98%
Methyl(naphthalen-2-yl)sulfane	7433-79-6	Adamas	98%
2-(Methylsulfinyl)naphthalene	35330-76-8	Bidepharm	95%

1. Wang, S.; Tang, L.; Cai, B.; Yin, Z.; Li, Y.; Xiong, L.; Kang, X.; Xuan, J.; Pei, Y.; Zhu, M., *J. Am. Chem. Soc.* 2022**, *144***, 3787-3792.

2. Zang, L. Y.; Zhang, Z.; Misra, H. P., *Photochem. Photobiol.* 2008**, *52***, 677-683.

3. Bregnhøj, M.; Westberg, M.; Minaev, B. F.; Ogilby, P. R., *Acc. Chem. Res.* 2017**, *50***, 1920-1927.

4. Grimme, S.; Antony, J.; Ehrlich, S.; Krieg, H., *J. Chem. Phys.* 2010**, *132***, 154104.

5. Marenich, A. V.; Cramer, C. J.; Truhlar, D. G., *J. Phys. Chem. B.* 2009**, *113***, 6378-6396.